

Multi-objective optimization design of the intake duct for a waterjet system

R F Huang^{1,2}, Y X Dai², Z H Zhai², Z Wang¹, J J Zhou² and X W Luo^{1*}

¹ State Key Laboratory of Hydroscience and Engineering, Tsinghua University, Beijing 100084, China

² Science and Technology on Water Jet Propulsion Laboratory, Shanghai 200011, China

Email: luoxw@mail.tsinghua.edu.cn

Abstract. An intake duct for a waterjet system is treated to improve the hydraulic efficiency and the outflow nonuniformity together with its perpendicularity. A multi-objective optimization strategy is proposed by incorporating with design of experiments (DOE), computational fluid dynamics (CFD), inverse design method, Kriging model and non-dominated sorting genetic algorithm-II (NSGA-II). Optimal Latin hyper-cube design method is used in DOE to uniformly sample in variation ranges, and global optimization is then conducted by using NSGA-II based on the input-target approximation functions approximated by the Kriging model. Instead of randomly selecting one solution to implement, a technique for ordering preferences by similarity to ideal solution (TOPSIS) is introduced to select the best compromise solution (BCS) from pareto-front sets. Compared with the original duct, the optimized intake duct has a much better outflow quality at the design operation point with a comparative hydraulic efficiency. Thus, the authors believe the proposed method is helpful for optimizing the intake duct.

1. Introduction

Waterjet propulsion is a preferred method to thrust high-speed marine vessels over 30 knots because of high propulsive efficiency, good maneuverability, less vibration and good anti-cavitation performance ^[1]. It consists of the intake duct, the pump, the nozzle and the steering device. The pump is the core component to transform the pressure energy into the kinetic energy at the nozzle exit and its efficiency is up to 90% with advanced modern design methods. In contrast, the intake duct upstream of the pump has lost about 7~9% of the shaft power ^[2] due to the local nonuniformity which results from the ingestion of the hull boundary layer, the shaft obstruction and the bend in the intake duct, etc., as reported by Bulten ^[3]. Besides, the propulsion efficiency is strongly affected by the interaction between the waterjet system and the hull, especially in the intake duct ^[4]. Thus, the optimization of the intake duct is necessary to improve the hydraulic efficiency and reduce the internal nonuniformity.

In the last decades, many investigations are devoted to the intake duct by experiments and computational fluid dynamics (CFD) technology. Esch ^[5] experimentally studied the effects of a nonuniform suction velocity profile on the hydrodynamics forces of the impeller by newly designing a dynamometer which was equipped with six full Wheatstone bridges of strain gauges to measure the six generalized force components, and found a backward whirling motion of the rotor system and a considerable steady radial force. Cao ^[6] numerically studied the performance deviation of a waterjet



pump between the uniform and nonuniform suction flows. Ding ^[7] proposed a parametric design method with sixteen geometrical parameters. If one geometrical parameter was changed, the others were automatically adjusted according to the geometrical constraints. Ji ^[8, 9] revealed that the duct efficiency was decreased with the increase of the incline angle and analysed the effects of lip parameters on the nonuniformity and the stagnation point.

In this paper, an intake duct of a waterjet propulsion system is treated to improve the hydraulic efficiency and the outflow nonuniformity together with its perpendicularity. A multi-objective optimization strategy is proposed in Section 2 by incorporating with design of experiments (DOE), computational fluid dynamics (CFD), inverse design method, Kriging model and non-dominated sorting genetic algorithm-II (NSGA-II). Section 3 provides performance comparisons between the optimized duct and the original duct, and the conclusions are given in Section 4.

2. Multi-objective optimization system

2.1. Decision variables and optimization objectives

The three-dimensional geometry of the intake duct is characterized with 13 parameters as shown in Figure 1. Generally, the duct diameter D , the total length L and the installation height H are subjected to the installation space in the marine vessels and the waterjet pump so that these three parameters are constant during our optimization design. Based on Ji's work ^[8, 9], the straight lines ($L1$, $L2$ and $L3$) have a little impact on the hydrodynamic performance so that they are treated as dependent variables and can be calculated by equations (1-4):

$$L1 + R1 \sin \alpha + L2 \cos \alpha + R2 \sin \alpha = L \quad (1)$$

$$R1(1 - \cos \alpha) + L2 \sin \alpha + R2(1 - \cos \alpha) = H + \frac{D}{2} \quad (2)$$

$$(R1 - D)(1 - \cos \alpha) + L3 \sin \alpha + R3 \cos \alpha + h = H - \frac{D}{2} \quad (3)$$

$$(R4 - h)^2 + (L3 \cos \alpha + (R1 - D - R3) \sin \alpha - (L - L0 - L1))^2 = (R4 - R3)^2 \quad (4)$$

where $R1=1.89D$ and $R4=1.0D$. Therefore, α , h , $R2$ and $R3$ are treated as host variables.

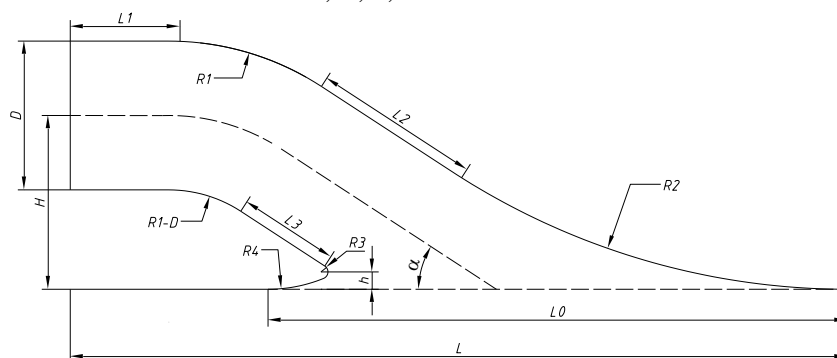


Figure 1. Characteristic parameters of the intake duct.

As recommended by 24th ITTC ^[10], the total energy is defined as $E_j = \int [0.5 \rho u_j^2 + (p_j - p_0) - \rho g x_j] dQ$, where E_j is the total energy at sectional plane j , g is the gravity acceleration, p_0 is the ambient pressure, Q is volume flux and ρ , u , x presents the fluid density, velocity, the local distance to the reference plane. Three parameters are used to evaluate the duct performance: hydraulic efficiency, $\eta = \frac{E_{out}}{E_{in}}$,

outflow nonuniformity, $\zeta = \frac{1}{Q} \int_{dA} |u_a - \bar{u}_a| dA$ and outflow perpendicularity, $\theta = \frac{1}{Q} \int_{dA} u_a \left[90^\circ - \arctan\left(\frac{u_t}{u_a}\right) \right] dA$,

where E_{out} is the total energy at the duct outflow plane, E_{in} is the total energy at the duct inlet plane positioned one impeller diameter forward of the ramp tangency point^[10], u_a is the axial velocity and u_t is the tangential velocity. Both the outflow nonuniformity and perpendicularity present the outflow quality of the intake duct that is the inflow profile to the impeller. In order to ensure the high efficient operation of the waterjet pump, outflow quality of the duct should be as good as possible. Therefore, the optimization objectives are to maximize the hydraulic efficiency and outflow perpendicularity and minimize the nonuniformity at the outflow plane.

2.2. Multi-objective optimization strategy

Figure 2 shows the flowchart of the multi-objective optimization which is combined with design of experiments (DOE), computational fluid dynamics (CFD), inverse design method, approximate method and non-dominated sorting genetic algorithm-II (NSGA-II). First of all, optimal Latin hypercube design method is introduced in DOE to uniformly sample in variation ranges. 75 tests are conducted with 8 input variables and three performance indexes are obtained with the CFD simulations. Subsequently, pareto-front sets are searched by using the non-dominated sorting genetic algorithm-II (NSGA-II) based on the input-target approximation functions obtained by the Kriging model. Instead of randomly selecting one solution to implement, a technique for ordering preferences by similarity to ideal solution (TOPSIS) is introduced to select the best compromise solution (BCS) that is not only shortest to the positive ideal solution but also longest to the negative ideal solution with objective weights computed by Shannon's entropy method.

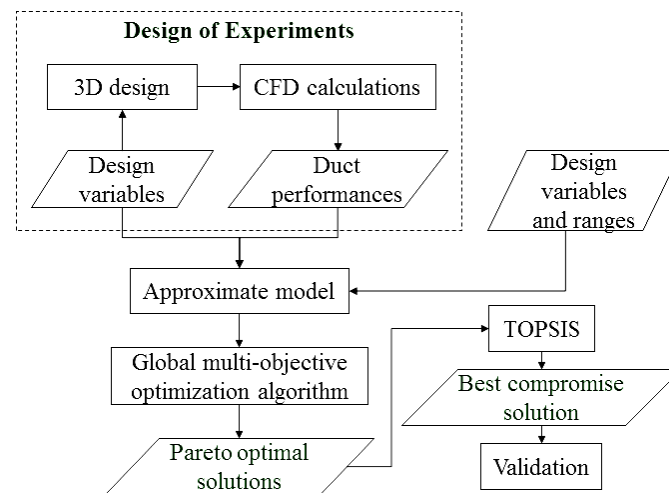


Figure 2. The multi-objective optimization flowchart.

2.3. CFD calculations

The SST $k-\omega$ turbulence model is used to simulate the internal flows in the intake duct since it can accurately predict the flow separation with considering the transport of the turbulent shear stress. Figure 3 shows the three-dimensional computational domain including the water tank, the intake duct and the barretter. The inlet of the water tank is $25D$ ahead of the intake duct with a $10D$ (width) \times $8D$ (height) cross section as recommended by Liu^[11]. The barretter is $10D$ in length for computational stability. Based on the mesh independence test, the final mesh has 4091921 nodes.

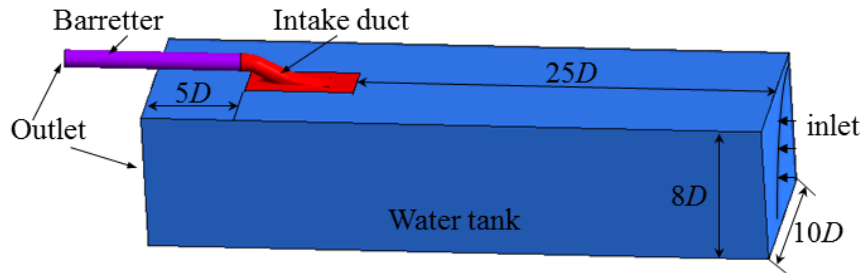


Figure 3. Computational domain.

As for the boundary conditions, a nonuniform velocity profile is set at the inlet of the water tank to simulate the development of the boundary layer along the hull surface, and it is defined in equation (5) [3], where u_a denotes the local axial velocity in the boundary layer at a distance y_r normal to the hull bottom, u_s is the ship speed, δ is the hull boundary layer thickness, L is the distance to the duct suction inlet, Re is Reynolds number. Free slip walls are applied at the bottom plane and the side planes of the water tank, so the mesh near these walls can be relatively coarse without resolving the boundary layer. The static pressure is assigned at the outlet plane of the water tank. The mass flow rate is set at the barretter outlet plane according to the inlet velocity ratio, $IVR = u_p / u_s$, where u_p denotes the averaged pump inlet velocity. The other solid walls are nonslip.

$$\begin{cases} u_a = u_s (y_r / \delta)^{1/9}, & y_r \leq \delta \\ u_a = u_s, & y_r > \delta \end{cases} \quad (5)$$

$$\text{where } \delta = 0.27LRe^{-1/6}$$

A high resolution scheme was set for the advection term with the turbulence numeric. The convergence criterion was 1×10^{-6} . All the calculations were conducted on servers with 12 Intel Xeon X5670 core processors and a 160G hard drive, which were supported by Tsinghua National Laboratory for Information Science and Technology.

3. Results and discussions

Figure 4 shows the pareto-front solutions during the globally multi-objective search by NSGA-II algorithm with 200 population size and 200 generations. The efficiency, outflow nonuniformity and perpendicularity are predicted by the Kriging model at this stage. Then, the best compromise solution marked in blue is determined by TOPSIS method among those pareto-front solutions. Details about the TOPSIS method refer to literature [12]. The weight of hydraulic efficiency, nonuniformity and perpendicularity at the outflow plane is 0.0018, 0.0132 and 0.9850, respectively, that is why BCS is more inclined to satisfy the outflow perpendicularity and nonuniformity.

The original and optimized ducts are shown in figure 5. table 1 shows the performance of the two ducts evaluated at the design ship speed and $IVR=0.7$ without considering effects of the rotating impeller and the obstruction of the flow due to the shaft. The predicted efficiency, outflow nonuniformity and perpendicularity obtained by Kriging model are in good agreement with those simulated by CFD technique. Compared with the original duct, the optimized duct has a much better outflow with $\theta=88.25^\circ$ and $\zeta=0.18$ although the efficiency is slightly decreased.

Pressure and velocity distributions at the midplane are depicted in figure 6, by using the pressure coefficient, $c_p = \frac{p - p_{ref}}{0.5\rho u_s^2}$ and dimensionless axial velocity, u_a / u_s , where p_{ref} denotes the reference pressure. During the suction process, the flows firstly strike the lip and go through the duct elbow. A small incline angle of the original duct results in the smooth flows inside without an obvious low-

pressure region. In contrast, the optimized duct with a large incline angle encounters a large area of low-pressure at the down side of the elbow which is likely to produce flow separations, causing a decrease in the hydraulic efficiency.

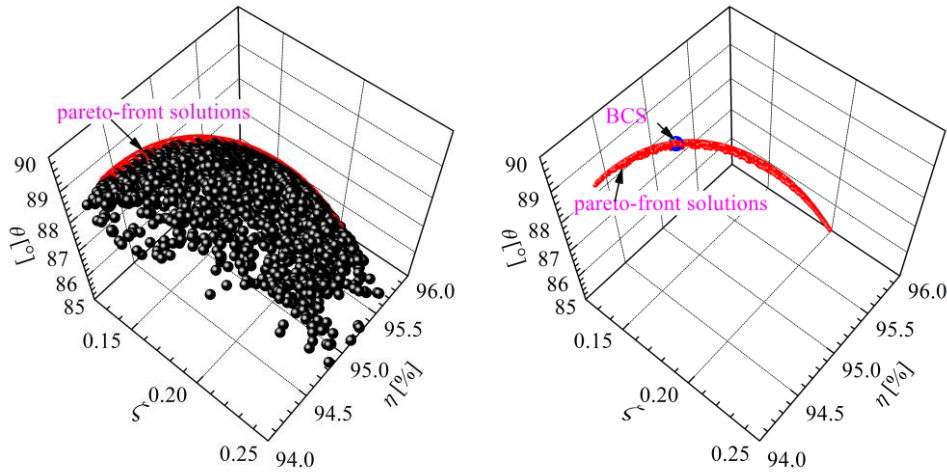


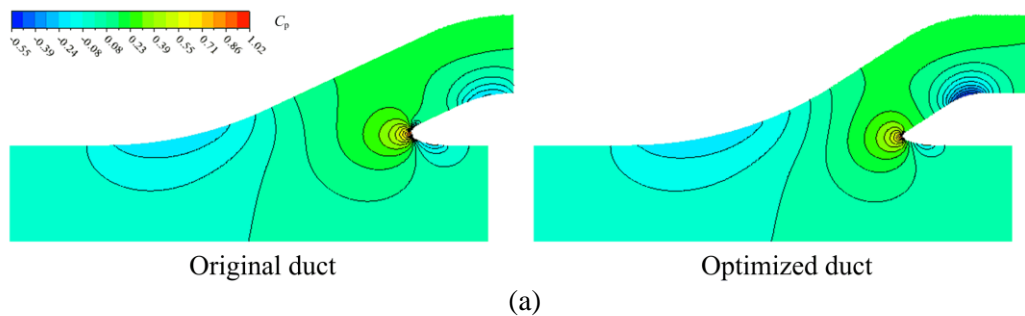
Figure 4. Pareto-front solutions and the best compromise solution (BCS).



Figure 5. Comparisons of the duct geometry (left-original duct, right-optimized duct).

Table 1. Performance comparisons between the original duct and optimized duct (IVR=0.7).

case	θ [°]	η [%]	ζ
approximate BCS	89.64	94.77	0.16
CFD BCS	88.25	94.91	0.18
original duct	85.60	95.05	0.22



(a)

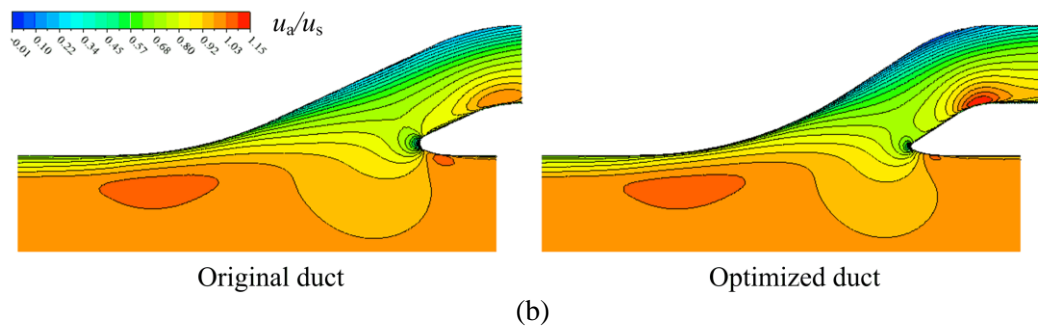


Figure 6. Pressure and velocity distributions at the midplane (IVR=0.7).

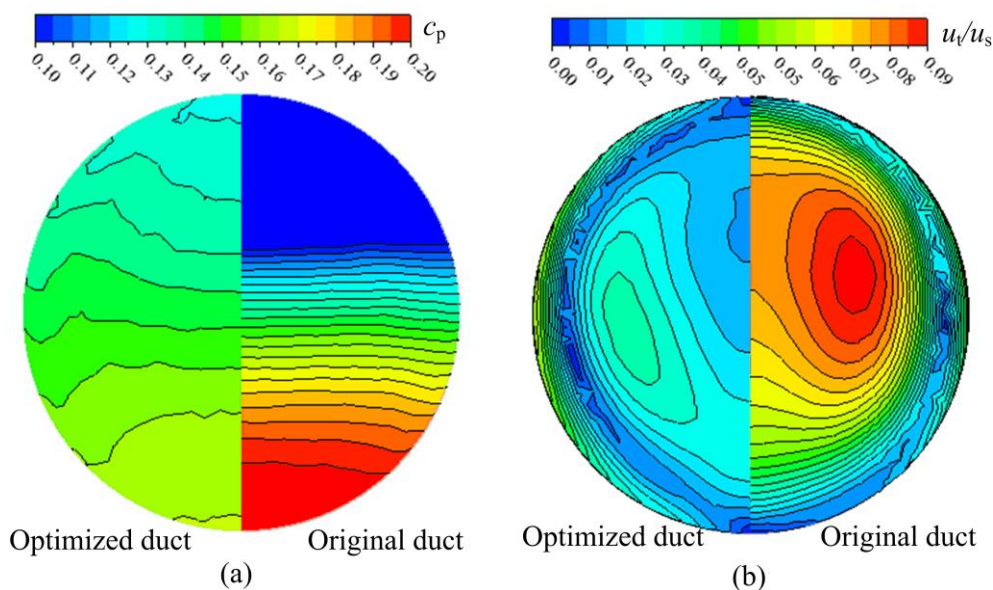


Figure 7. Pressure and velocity distributions at the outlet plane of the intake duct (IVR=0.7).

Figure 7 shows distributions of the pressure and tangential velocity (u_t/u_s) at the outlet plane of the intake duct (IVR=0.7). The optimized duct shows a much uniform pressure distribution at the exit plane while the original duct suffers from a low-pressure region at the downside and a high-pressure region at the upside. In terms of the secondary flows at the exit plane, the optimized duct performs much uniform while an intensive region of the high tangential velocity shows in the original duct.

4. Conclusions

This paper proposes a multi-objective optimization system which consists of design of experiments (DOE), computational fluid dynamics (CFD), inverse design method, Kriging model and non-dominated sorting genetic algorithm-II (NSGA-II). Optimal Latin hyper-cube design method is used in DOE to uniformly sample in variation ranges, and global optimization is then conducted by using NSGA-II based on the input-target approximation functions approximated by the Kriging model. Instead of randomly selecting one solution to implement, a technique for ordering preferences by similarity to ideal solution (TOPSIS) is introduced to select the best compromise solution (BCS) from pareto-front sets.

An intake duct for a waterjet system is optimized using this proposed system. The geometry is characterized with 13 parameters and the optimization objectives are the hydraulic efficiency, the outflow nonuniformity and perpendicularity. As a result of the optimized duct, the outflow nonuniformity is decreased by 18% and the outflow perpendicularity is increased by 3% with a slight

decrease by 0.15% in hydraulic efficiency. Further study is expected to improve hydraulic efficiency of the optimized duct.

Acknowledgments

This work was financially supported by National Natural Science Foundation of China (Project Nos. 51376100 and 51776102), the State Key Laboratory for Hydrosience and Engineering (Project No. 2017-E-02) and Tsinghua National Laboratory for Information Science and Technology.

References

- [1] Park W G, Jang J H, Chun H H and Kim M C 2005 Numerical flow and performance analysis of waterjet propulsion system *Ocean Eng* 32 1740-61
- [2] Park W G, Yun H S, Chun H H and Kim M C 2005 Numerical flow simulation of flush type intake duct of waterjet *Ocean Eng* 32 2107-20
- [3] Bulten N W H 2006 Numerical analysis of a waterjet propulsion system (Technische Universiteitindhoven)
- [4] Terwisga T and van 1991 The effect of waterjet-hull interaction on thrust and propulsive efficiency *Waterjet Propelled Craft*
- [5] Van Esch B P M 2009 Performance and radial loading of a mixed-flow pump under non-uniform suction flow *J Fluids Eng Trans ASME* 131 0511011-7
- [6] Cao P, Wang Y, Kang C, Li G and Zhang X 2017 Investigation of the role of non-uniform suction flow in the performance of water-jet pump *Ocean Eng* 140 258-69
- [7] Ding J and Wang Y S 2010 Parametric design and application of inlet duct of marine waterjet *Journal of Shanghai Jiaotong University* 44 1423-8
- [8] Ji G R, Cai Y L, Li N and Yu Y 2016 Influence of lip parameters on non-uniformity and stagnation point at inlet duct of waterjet propulsion *Shipbuilding of China* 57 109-15
- [9] Ji G R, Cai Y L, Li N, Yin X H and Yu Y 2016 Analysis about affect of inclination angle on the efficiency of the waterjet propulsion inlet duct *Ship Science and Technology* 38 55-8
- [10] Navale A, George J and Iii H 2004 The specialist committee on validation of waterjet test procedures final report and recommendations to the 24th ITTC
- [11] Liu C J, Wang Y S, Zhang Z H and Liu J B 2010 Research on effect of different flow control volume on waterjet performance prediction *Journal of Ship Mechanics* 14 1117-21
- [12] Huang R F, Luo X W, Ji B, Wang P, Yu A, Zhai Z H and Zhou J J 2015 Multi-objective optimization of a mixed-flow pump impeller using modified NSGA-II algorithm *Sci. China Technol. Sci.* 1-9